UDC 538.915

L.G. Gerchikov[1], Yu.A. Mamaev[1], Yu.P. Yashin[1], V.V. Kuz'michev[1], K. Aulenbacher[2], E. Riehn[2]

[1] St. Petersburg State Polytechnical University
29 Politekhnicheskaya St., St. Petersburg, 195251, Russia
[2] Institute of Nuclear Physics, Johannes Gutenberg University
Saarstraße 21, 55122 Mainz, Germany.

ELECTRONIC TRANSPORT IN STRAINED AlInGaAs/AlGaAs SUPERLATTICES

Л.Г. Герчиков, Ю.А. Мамаев, Ю.П. Яшин, В.В. Кузьмичев, К. Ауленбахер, Э. Райх

ЭЛЕКТРОННЫЙ ТРАНСПОРТ В НАПРЯЖЕННЫХ СВЕРХРЕШЕТКАХ AlInGaAs/AlGaAs

Transport of spin polarized electrons in semiconductor AlInGaAs/AlGaAs superlattices (SL) with strained quantum wells used for photoemitter application is studied. The experimental study is based on the time resolved measurements of electron emission from the cathode after its photoexcitation by fs laser pulse. We report the variation of the SL response time with the number of superlattice periods. We have also performed theoretical calculations of photocathode pulse response and compared the obtained results with experimental data. Our analysis testifies the presence of partial electron localization in SL. We demonstrate that electron localization suppresses electronic transport and strongly limits the cathode quantum efficiency.

SUPERLATTICE, DFIFFUSION, PHOTOEMISSION, ELECTRONIC TRANSPORT.

Экспериментально и теоретически исследован транспорт поляризованных электронов в фотокатодах на основе полупроводниковой, сильно напряженной сверхрешетки. Экспериментальное исследование основано на измерении с разрешением по времени электронной эмиссии из фотокатода после его фотовозбуждения фемтосекундным лазерным импульсом. Экспериментально определены времена фотоотклика сверхрешеток с различным числом периодов. Проведены расчеты фотооклика катодов и результаты сопоставлены с экспериментальными данными. Сделан вывод о наличии в свехрешетке частичной локализации фотоэлектронов. Показано, что электронная локализация подавляет электронный транспорт и сильно ограничивает квантовую эффективность фотокатодов.

СВЕРХРЕШЕТКА, ДИФФУЗИЯ, ФОТОЭМИССИЯ, ЭЛЕКТРОННЫЙ ТРАНСПОРТ.

I. Introduction

At the present time strained semiconductor superlattices (SL) are known as most effective basis of highly polarized electron sources [1]. Such photoemitters combine the advantages of conventional polarized electron sources based on a strained semiconductor layer with additional possibilities for band structure engineering of photocathode working layers based on strained SL. The major goal of SL development for photoemitter applications in the past decade was the achievement of electron polarization more than 90 %. For this purpose several types of SLs with highest possible valence band splitting have been developed, namely the SLs with strained quantum wells (QW) [2, 3] and with strained barriers [4]. Valence band splitting in SL, i. e. the energy splitting between the upper heavy and light hole minibands, is formed due to the combination of two effects: the strain deformation of SL layers and the quantum confinement. The aim of the optimal SL design is to provide a valence band splitting of more

than 70–80 meV together with good transport properties and high structural quality.

However, the significant progress in electron polarization was achieved at the expense of the quantum efficiency (QE) which does not exceed 1 % at the polarization maximum. Indeed, the maximum spin polarization of photoelectrons takes place at the photoabsorption threshold where the photoabsorption coefficient is rather small. Strained SL cannot be made too thick due to the possible strain relaxation resulting in structural defects, smaller residual strain and lower polarization. The best combination of polarization P = 92 % and QE = 0.85 % has been achieved for AlInGaAs/AlGaAs SL with strained QWs [3]. Thus, the further progress of polarized electron sources based on semiconductor SLs is shifted towards the developing highly effective photoemitters in order to meet the modern requirements of high energy physics [5].

Our study demonstrates that simple increase of the SL thickness does not lead to increase of QE like it is observed in the case of conventional photoemitters with GaAs working layer [6, 7]. In order to understand this surprising phenomenon, we perform the time resolved measurements of electron emission from the cathodes after their excitation by fs laser pulse. This method has been developed by K. Aulenbacher et al. [6] while studying the spin polarized electron transport in conventional photocathodes. The series of AlInGaAs/AlGaAs SLs containing from 6 to 15 periods have been fabricated and studied. In all samples we observe two exponential decays of electron emission, which indicates the presence of partial electron localization in a SL. The fast decay is caused by electron emission from the first electronic miniband while slow response decay is connected with electrons trapped by the localized states.

We also developed a theoretical description of electron transport in a SL based on the time dependent kinetic equation and calculated the photocathode pulse response [8]. The obtained results are in a good agreement with the experimental observations. The employed model determines the time of electron transport in SL, electron capture and detachment times, portion of photoelectrons that have been localized by the traps in SL and corresponding losses of QE.

II. Experiment

We have studied the pulse response of six photocathodes based on AlInGaAs/AlGaAs SL with strained QWs. All samples were grown on a p-type (100) GaAs substrate by molecular beam epitaxy (MBE). The cathode structure contains a thick $Al_xGa_{1-x}As$ (x = 0.35 – 0.40) buffer layer that is p-doped by beryllium to the level $6{\cdot}10^{18}$ cm^{-3}. On the top of the buffer, the cathode working layer was grown containing 6 to 15 periods of $Al_xIn_yGa_{1-x-y}As(a)$/$Al_zGa_{1-z}As(b)$ SL p-doped to a lower level of $3{\cdot}10^{17}$ cm^{-3}. Layer composition, x, y, z, values of the QW– (a) and barrier- (b) layer thickness as well as the number of SL periods (N) are shown in Table 1. Above the SL, a 6 nm GaAs

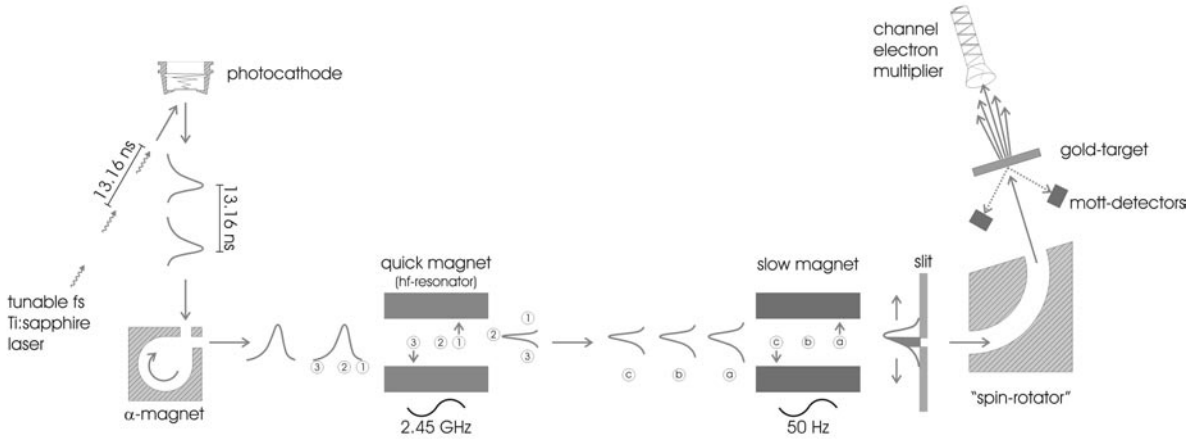

Fig. 1. Experimental setup

Table 1

Composition of photocathode working layers

Sample	QW		Barrier	Thickness		Period
	x, %	*y*, %	*z*, %	*a*, nm	*b*, nm	*N*
SL 5-998	20	16	28	3.5	4.0	15
SL 5-337	20	16	28	5.0	4.0	15
SL 7-395	20	19	40	5.4	2.1	12
SL 7-396	20	19	40	5.4	2.1	12
SL 6-905	20	15.5	36	5.1	2.3	10
SL 6-908	20	15.5	36	5.1	2.3	6

Values given: Number of SL periods (N), concentration of Al (x) and In (y) in $Al_xIn_yGa_{1-x-y}As$ QW layer; Al concentration (z) in $Al_zGa_{1-z}As$ barrier layers and their thicknesses (a – QWs, b – barriers).

heavily Be-doped to the level of $7\cdot10^{18}$ cm^{-3} ($1\cdot10^{19}$ cm^{-3} for SL 5-998) surface layer was grown to produce thin band bending region (BBR). Finally, the GaAs surface was activated by repeated deposition of cesium and oxygen to achieve the negative electron affinity. All the experiments were performed at room temperature.

The experimental setup is shown in Fig. 1. The electron pulses are generated by an approximately 150 fs long laser pulse from a titanium-sapphire laser. An increase of pulse length to 300 fs takes place during optical beam transport to the cathode. These light pulses are synchronized to the output of a klystron which drives a 2.45 GHz-deflection cavity. By passing the first deflection cavity (quick magnet in Fig. 1), the longitudinal profile of the electron bunches is transferred into a corresponding transverse profile. The pulse profile can then be measured by moving the electron pulse in the second deflection cavity (slow magnet in Fig. 1) over a narrow slit and detecting the transmitted current. By analyzing the spin polarization of the transmitted electrons with a Mott polarimeter, a time resolved polarization measurement is obtained. The details of the apparatus are described in [6].

III. Theory

We describe the electron transport in a SL by means of the time dependent kinetic equation:

$$\frac{\partial\hat{\rho}}{\partial t} = -\frac{i}{\hbar}\left[\hat{H}\hat{\rho}\right] + I\{\hat{\rho}\}. \qquad (1)$$

Here ρ is the electron density matrix, $\hat{H}$ is the effective electron Hamiltonian for the first electronic miniband $e1$ which describes the quantum electron motion along SL axis. The collision term $I\{\rho\}$ on the right-hand side of Eq.(1) takes into account all the processes of electron scattering on impurities and phonons, the processes of photoexcitation, recombination and electron extraction into BBR.

We calculate the miniband energy spectrum using the multiband Kane model, including the conduction band Γ_6, the states of light and heavy holes of the valence band Γ_8 and also the states of the spin-orbit splitted Γ_7 band [9]. The width ΔE of the $e1$ miniband along the SL axis in the considered samples is in the range 20–40 meV. These values are much smaller than the conduction band offsets which appear to be larger than 200 meV for all considered samples. Consequently, the vertical electron motion along SL axes can be well described within the tight binding approximation. For effective Hamiltonian $\hat{H}$ it means that we have to take into account the coupling matrix element $V \equiv H_{n,n+1} = \Delta E/4$ between the neighboring QWs only. This matrix element determines the tunneling time between neighboring QWs $\tau_{QW} = \pi\hbar/2V = 2\pi\hbar/\Delta E$ which is about 100 fs for our samples. The total time of ballistic motion through the SL containing N QW amounts to $\tau_{SL} = 2\pi\hbar N/\Delta E$.

Taking into account the transition matrix elements for the neighboring QW only, the kinetic equation (1) for electron population of each QWs, i. e. for the diagonal elements ρ_{nn} of density matrix, is written as

$$\frac{\partial \rho_{nn}}{\partial t} = -\frac{2V}{\hbar}\,\mathrm{Im}\{\rho_{n,n+1}\} + \frac{2V}{\hbar}\,\mathrm{Im}\{\rho_{n-1,n}\} + I\{\hat{\rho}\}_{nn}. \quad (2)$$

The first two terms in the right-hand side of Eq.(2) corresponds to the electron currents from n-th QW to two neighboring QWs with the numbers $n + 1$ and $n - 1$, respectively.

The diagonal elements of the collision term $I\{\rho\}$ on the right-hand side of Eqs. (1), (2) are connected with photoexcitation and recombination processes. Calculation of the photogeneration rate is described in details in Ref. [9]. The recombination contribution to the collision term is given by the diagonal matrix element ρ_{nn}/τ_r, where τ_r is the electron recombination time. For the final N-th QW close to the BBR, there is an additional contribution connected with electron tunneling to the BBR. Corresponding electron extraction current I can be written via the number of electrons in the last QW, ρ_{NN}, and tunneling time through the last barrier τ_f:

$$I = \frac{\rho_{NN}}{\tau_f}. \quad (3)$$

The non-diagonal density matrix elements $\rho_{nn'}$ and corresponding electron currents between the neighboring QWs in Eq. (2) are determined by transition matrix element V and non-diagonal elements of the collision term $I\{\hat{\rho}\}_{nn'}$. The last ones we will right within the constant relaxation time approximation:

$$I\{\hat{\rho}\}_{nn'} = -\hat{\rho}_{nn'} / \tau_p. \quad (4)$$

Due to the weak coupling between the neighboring QWs, the momentum relaxation time τ_p is mostly determined by the processes of electron scattering within each QW layer. In the stationary case, in approximation accounting for the neighboring QWs only, it follows from Eqs. (1), (4) that

$$\rho_{n,n+1} = -i\frac{V\tau_p}{\hbar}(\rho_{n+1,n+1} - \rho_{nn}). \quad (5)$$

Consequently, the electron current from n-th to $(n + 1)$-th QW is equal to

$$I_{n,n+1} = \frac{2V}{\hbar}\,\mathrm{Im}\{\rho_{n,n+1}\} = -\frac{2V^2\tau_p}{\hbar^2}(\rho_{n+1,n+1} - \rho_{nn}). \quad (6)$$

For numerical calculations, we take the momentum relaxation time equal to $\tau_p = 75$ fs. Note that τ_p is comparable to the time of free electron tunneling between neighboring QWs τ_{QW}. Therefore, electron transport along SL axis is diffusion, not the ballistic motion.

To calculate the tunneling time from SL to BBR τ_f, we solve the separate quantum mechanical problem of free electron motion through the single QW to BBR [8]. It is worth noting that the obtained τ_f is larger than the tunneling time between neighboring QWs τ_{QW}, e. g. for SL 5-998 $\tau_f = 0.25$ ps while $\tau_{QW} = 0.1$ ps. It is quite natural because the tunneling between the neighboring QWs is a resonant process and its probability is proportional to the first order of the tunneling exponent $\exp(-\kappa b)$, where κ is the electronic wave vector under the barrier and b is the barrier width. The tunneling through the last barrier is a non-resonant process and its probability is much smaller since it is proportional to the second order of the tunneling exponent $\exp(-2\kappa b)$. Hence, the total time of electron motion from SL to BBR is mainly determined by the slowest process, i. e. by the tunneling through the last barrier.

Eq. (3) can be considered as the boundary condition at the SL/BBR interface. At the opposite side of SL, i. e. at the buffer interface, the electron current is equal to zero, $I = 0$. In the case of electron diffusion in the bulk sample, the boundary conditions are usually written via the surface recombination velocity $S = j/n$, where j is the diffusion current density and n is the electron concentration. Since electron current in buffer layer is zero, we assume zero surface recombination velocity $S = 0$ at the buffer interface. At the opposite side of working layer, at the BBR interface, the surface recombination velocity, according to Eq.(3), is equal to

$$S = \frac{d}{\tau_f}, \quad (7)$$

where $d = a + b$ is the SL period.

Surface recombination velocities for our SL based cathodes calculated according to Eq. (7) are smaller than in the case of con-

ventional photoemitters. For example, in case of SL 5-998, $S = 3 \cdot 10^6$ cm/s, for SL 6-905 $S = 5 \cdot 10^6$ cm/s while in the bulk GaAs $S = 10^7$ cm/s [6, 7].

For numerical simulation of the cathode response, we solve the time-dependent kinetic Eq. (1) with time dependence of the laser pulse intensity described by the Gaussian profile. The obtained electron current $I(t)$ (3) is compared to the experimental pulse response (see next section). The calculated pulse response exponentially decays with time, and we define the corresponding decay time as electron transport time τ_t. It is possible, however, to derive the approximate analytical expression for τ_t. In the steady state under the stationary pumping, kinetic Eq. (1) has an analytical solution (Eqs.(5, 6)), which is correct if the miniband width ΔE is smaller than the photoelectron energy distribution. The transport time defined in the stationary case as the ratio of number of electrons inside the SL to the generation rate, $\tau_t = \sum_{n=1}^{N} \rho_{nn} / I$, $I = I_{n,n+1}$, is equal to

$$\tau_t = \frac{\hbar^2 (N - 1/2)(N-1)}{6|V|^2 \tau_p} + N\tau_f. \qquad (8)$$

According to Eq. (8), the transport time is a sum of the diffusion time within the SL given by the first term on the right-hand side, and the time $N\tau_f$, taken to penetrate through the last barrier to the BBR. For the twelve-period SL 5-998, Eq.(8) gives the transport time $\tau_t = 5$ ps. The main contribution, 3 ps, comes from the tunneling through the last barrier to BBR.

Note that in the limit of thick SL, $N >> 1$, Eq. (8) transfers into a corresponding expression of the standard diffusion model in the bulk sample:

$$\tau_t = \frac{L^2}{3D} + \frac{L}{S}, \qquad (9)$$

where $L = Nd$ is the SL length.

The surface recombination velocity S is given by Eq. (7), and diffusion coefficient D of SL is equal to

$$D = \frac{2|V|^2 d^2 \tau_p}{\hbar^2}. \qquad (10)$$

The typical value of D is about 15 cm^2/s, e. g. for SL 5-998 $D = 12$ cm^2/s and for SL 6-905 $D = 17$ cm^2/s. It is a few times smaller than the diffusion coefficient $D = 40$ cm^2/s in the bulk GaAs [6, 7].

Our calculations of the cathode QE and pulse response according to the kinetic scheme described above revealed the significant discrepancy between experiment and theory. Namely, theory predicts the gradual increase of QE with the growth of SL thickness up to the hundreds nanometers while such increase actually saturates at few tens nanometers thicknesses (see the next section). Then, the theory predicts the simple exponential decay of pulse response with time described by Eq. (8), while the experimental signal reveals a non-exponential decay (see the next section). These facts indicate the presence of partial electron localization in a SL. That is why we include in the density matrix ρ the localized electron states besides the delocalized miniband states and introduce in the collision term $I\{\hat{\rho}\}$ processes of electron capture and detachment with characteristic times τ_c and τ_d respectively. We do not consider transitions between electron states localized within the different QWs, because such transitions are non-resonant and hence they are very slow compared to the interwell transitions via miniband states described by Eq.(6). Coupling between the localized and delocalized (miniband) states occurs via capture and detachment processes within each QW. In the extended kinetic scheme accounting for the partial electron localization, these processes are described by the diagonal matrix elements in the collision term $\rho_{nm,nm}/\tau_c$ and $\rho_{nl,nl}/\tau_d$, for capture and detachment, respectively. Here indexes m and l after the QW number n in the density matrix subscripts indicate whether the electron state is miniband or localized, respectively.

IV. Results and Discussion

We have measured QE for series of cathodes based on SL with composition close to SL 6-905 and containing from 2 to 20 periods. The results are presented in Fig. 2. The significant scattering of experimental data is connected with large variation of electron emission probability from BBR to the vacuum via cathode surface activated with Cs–O. This feature of

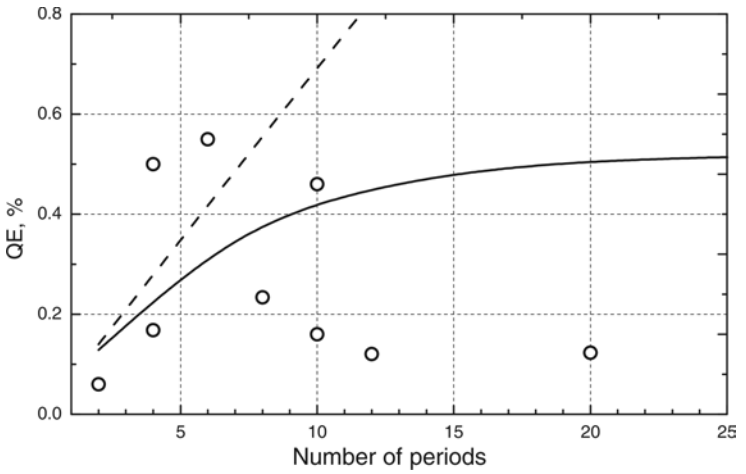

Fig. 2. Quantum efficiency dependence on SL thickness.
Open dots show the experimental results. Solid and dashed lines show the theoretical results calculated with and without electron localization, respectively

experimental data impedes the detailed comparison between the experiment and theory. Nevertheless, one can conclude that the experimental measurements do not support the linear increase of QE calculated without accounting for electron localization (dashed line). The influence of electron localization is shown by solid line which has been calculated assuming partial electron localization. It demonstrates that electron localization strongly suppresses the QE increase. The parameters of electron localization used for these calculations are shown in Table 2 for SL 6-905 sample. Their choice will be discussed below. The electron recombination time in SL was taken τ_r = 50 ps [10].

The more detailed study of electron transport in the considered nanostructures was done by means of time resolved pulse response measurements. For all considered samples presented in Table 1, we calculated the pulse response by the numerical solution of Eq. (1). The obtained results, together with the experimental data, are shown in Fig. 3 and presented in Table 2. The dashed lines in Fig. 3 show the pulse response calculated without electron localization. It exponentially decays with the decay time equal to the time of miniband electron transport τ_t quite close to the approximate Eq. (8). The calculated miniband electron times τ_t are presented in the third column of the Table 2. Fig. 3 demonstrates that in all samples experimental signal decays faster than τ_t. We interpret this fact

Table 2

Parameters of vertical electron transport

Sample	Number of periods	Miniband transport time, ps	Capture time, ps	Detachment time, ps	Response time, ps	Diffusion length, periods	Electron losses, %
SL 5-998	15	5.8	4.5	6.0	2.3	36	12
SL 5-337	15	15.8	5.5	160	4.0	8	64
SL 7-395	12	4.5	3.7	200	2.1	11	45
SL 7-396	12	4.5	9.0	110	3.0	18	23
SL 6-905	10	2.5	2.1	130	1.1	10	41
SL 6-908	6	1.2	4.5	50	0.95	19	9

Values given: Transport time of *e*1 miniband (τ_t), capture time (τ_c), detachment time (τ_d), response time (τ), diffusion length and losses of photoelectrons SL.

as an evidence of partial electron localization. Indeed, in the presence of electronic traps, the electron current will decay faster due to combination of two processes: electron transport from SL to BBR with subsequent emission into the vacuum and electron capture by the traps. Roughly, the decay (or response) time can be approximated as $\tau = 1/(1/\tau_{t.} + 1/\tau_{c.})$. The resulting response times are presented in the sixth column of the Table 2. The solid lines in Fig. 3 show the pulse response calculated taking into account electron capture and reverse detachment processes. Fig. 3 demonstrates quite good agreement of the experiment and theory. The capture and detachment times are used as fitting parameters, and their values are shown in Table 2. These times depend on the trap density and strongly vary from one sample to another. This fact masks the response time dependence on the number of SL periods. Thus six (SL 6-908) and ten (SL 6-905) period samples have close response times though the miniband transport time of the longer SL is more than two times larger than for the shorter one.

Samples with shorter capture and larger detachment times have the larger level of electron localization. In these samples electron transport is suppressed because considerable part of photoelectrons is localized by the traps and have low chance to escape to BBR prior to recombination. To demonstrate the effect of localization on QE, we show in the last two columns of Table 2 the diffusion length $L_D = (D\tau_r)^{1/2}$ and electronic losses in SL. In the samples with high localization level, the diffusion length is comparable with SL thickness, which in turn leads to considerable electronic losses. This fact explains why QE does not increase with the growth of SL thickness. The increase of the SL thickness beyond the diffusion length just leads to needless electronic losses. It is demonstrated by the solid curve in Fig. 2 calculated with the following parameter of SL 6-905 sample: $L_D/d = 10$.

The sample with the best transport properties is SL 6-908. It has the largest ratio of diffusion length to SL thickness $L_D/L = 3$ and consequently the lowest electronic losses. If all the

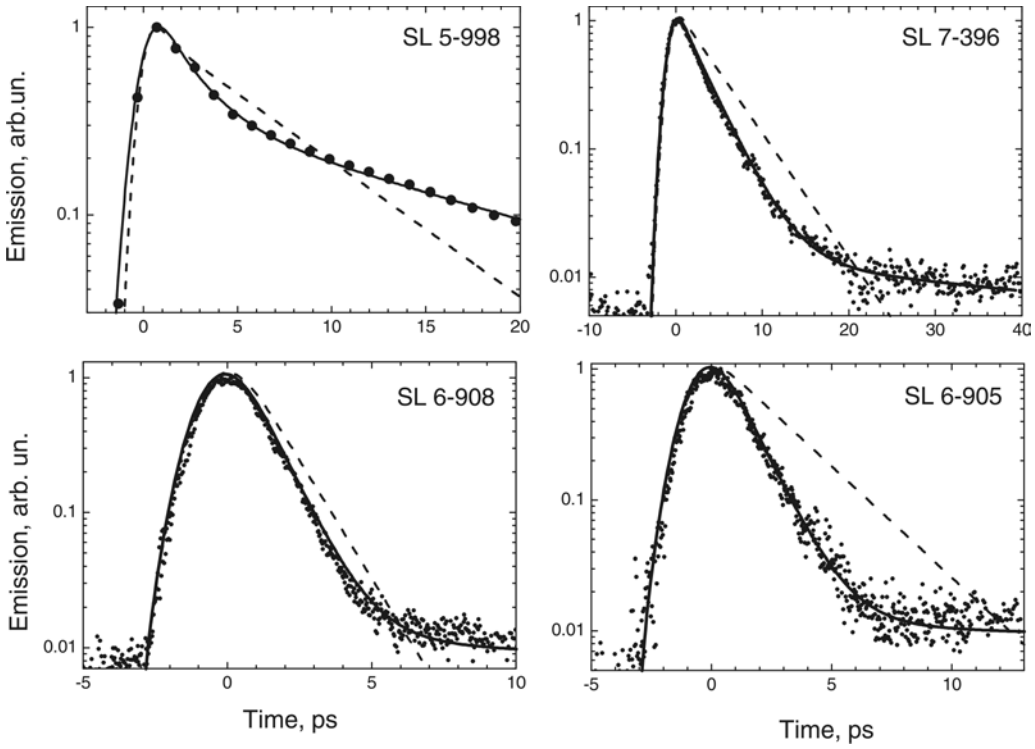

Fig. 3. Pulse response of SL 5-998, SL 7-396, SL 6-905 and SL 6-908 samples. Experimental signal is shown by dots, solid and dashed lines show the pulse response calculated with and without partial electron localization respectively

electrons in SL 6-908 are delocalized, the ratio L_D/L should be equal to 6.5. Roughly, this ratio indicates how QE can be enhanced if one is able to fabricate the cathode with SL thickness beyond L_D keeping the constant SL transport properties. However, our study shows that longer SLs have worse transport properties, e. g. SL 6-905 compared to SL 6-908.

Within the present work, we do not determine the nature of the localized electronic states as well as possible dependence of their density on SL thickness. The photocathode structure is heavily *p*-doped in order to achieve thin BBR. The highest doping level about 10^{19} cm^{-3} is applied in BBR, but the working layer is also heavily doped up to $3{\cdot}10^{17}$ cm^{-3}. Fluctuations of impurity potential might be responsible for the formation of localized electron states. Such phenomena have been observed earlier in GaAs/AlAs SLs at a comparable doping level of $1{\cdot}10^{17}$ – $7{\cdot}10^{17}$ cm^{-3} [11]. The 60 % of localized states in the lowest electron miniband e1 at the doping level of $4{\cdot}10^{17}$ cm^{-3} have been reported. The drop of vertical electron conductivity caused by partial electron localization was observed.

Unavoidable fluctuations of the layer composition and thicknesses can also contribute to partial electron localization. However, one can assume that the density of electronic traps formed due to these mechanisms should not depend on the SL length. On the contrary, the density of structural defects such as dislocations formed in SLs due to the strain relaxation, increases with the thickness of SLs. Lattice mismatch deformation of the QW layers shifts the conduction band edge upwards by approximately 0.1 eV. Thus, the deformation potential of dislocation plays a role of deep well for miniband electrons and can form the localized electron states. Note that the strong deformation of the SL is needed to produce sufficient energy splitting between light- and heavy-hole minibands to achieve high electron polarization. Further work will be focused on the nature of electron localization. Its main goal will be to determine the maximal number of SL periods that can be grown keeping good transport properties in combination with high electron polarization.

V. Conclusions

The pulse response of series of photocathodes with AlInGaAs/AlGaAs SLs with different numbers of periods has been studied. The analysis performed argues the presence of partial electron localization in SLs. The proposed kinetic model taking into account transport of miniband electrons from a SL to BBR, their capture by electronic traps and the reverse detachment process provides a good agreement between experimental findings and theoretical results. We demonstrate that electron localization slows down electron transport and leads to detrimental losses of photoelectrons. Partial electron localization limits maximal QE and useful thickness of SL based cathode working layer.

This work was supported by DFG through SFB 443.

REFERENCES

1. **Subashiev A.V., Mamaev Yu.A., Yashin Yu.P., Clendenin J.E.** Spin-polarized electrons: generation and applications. *Phys. Low-Dimentional Structures.* 1999, Vol. 1/2, pp. 1–36.

2. **Nishitani T., Nakanishi T., Yamamoto M., Okumi S., Furuta F., Miyamoto M., Kuwahara M., Yamamoto N., Naniwa K., Watanabe O., Takeda Y., Kobayakawa H., Takashima Y., Horinaka H., Matsuyama T., Togawa K., Saka T., Tawada M., Omori T., Kurihara Y., Yoshioka M., Kato K., Baba T.** Highly polarized electrons from GaAs-GaAsP and InGaAs-AlGaAs strained-layer superlattice photocathodes. *J. Appl. Phys.,* 2005, Vol. 97, p. 94907.

3. **Mamaev Yu.A., Gerchikov L.G., Yashin Yu.P., Vasiliev D.A., Kuzmichev V.V., Ustinov V.M., Zhukov A.E., Mikhrin V.S.** Optimized photocathode for spin-polarized electron sources. *Appl. Phys. Lett.,* 2008, Vol. 93, pp. 81114–81116.

4. **Gerchikov L.G., Mamaev Yu.A., Subashiev A.V., Yashin Yu.P., Vasil'ev D.A., Kuz'michev V.V., Zhukov A.E., Semenova E.S., Vasil'ev A.P., Ustinov V.M.** Photoemission of polarized electrons from InAlGaAs/GaAs superlattices with minimum conduction band offsets. *Semiconductors*, 2006, Vol. 40, pp.1326–1332.

5. **Brachmann A., Clendenin J.E., Garwin E.L., Ioakeimidi K., Kirby R.E., Maruyama T., Prescott C.Y., Sheppard J., Turner J., Zhou F.** The polarized electron source for the International Collider

(ILC) Project. *AIP Conference Proceedings of 17th International Spin Physics Symposium* (Kyoto, Japan, 2–7 October 2006), 2007, Vol. 915, pp. 1091–1094.

6. **Aulenbacher K., Schuler J., v. Harrach D., Reichert E., Roethgen J., Subashev A., Tioukine V., Yashin Y.** Pulse response of thin III/V semiconductor photocathodes. *J. Appl. Phys.,* 2002, Vol. 92, pp. 7536–7543.

7. **Oskotskij B.D., Subashiev A.V., Mamaev Yu.A.** Polarized photoemission spectra of the strained semiconductors layers. *Phys. Low-Dim. Struct.,* 1997, Vol. 1/2, pp. 77–89.

8. **Gerchikov L.G., Aulenbacher K., Mamaev Yu.A., Riehn E.J., Yashin Yu.P.** Transport and partial localization of electrons in strained short-period semiconductor superlattices. *Semiconductors,* 2012, Vol. 46, pp. 67–74.

9. **Subashiev A.V., Gerchikov L.G., Ipatov A.I.** Optical spin orientation in strained superlattices. *J. Appl. Phys.*, 2004, Vol. 96, pp. 1511–1520.

10. **Matsuyama T., Takikita H., Horinaka H., Wada K, Nakanishi T., Okumi S., Nishitani T., Saka T., Kato T.** High spin polarization of conduction band electrons in GaAs-GaAsP strained layer superlattice fabricated as a spin-polarized electron source. *Jap. J. Appl. Phys.*, 2004, Vol. 43, pp. 3371–3375.

11. **Pusep Yu.A., Chiquito A.J., Mergulhao S., Galzerani J.C.** One-dimensional character of miniband transport in doped GaAs/AlAs superlattices. *Phys. Rev. B,* 1997, Vol. 56, pp. 3892–3895.

СПИСОК ЛИТЕРАТУРЫ

1. **Subashiev A.V., Mamaev Yu.A., Yashin Yu.P., Clendenin J.E.** Spin-polarized electrons: generation and applications. *Phys. Low-Dimentional Structures.*, 1999. Vol. 1/2, pp. 1–36.

2. **Nishitani T., Nakanishi T., Yamamoto M., Okumi S., Furuta F., Miyamoto M., Kuwahara M., Yamamoto N., Naniwa K., Watanabe O., Takeda Y., Kobayakawa H., Takashima Y., Horinaka H., Matsuyama T., Togawa K., Saka T., Tawada M., Omori T., Kurihara Y., Yoshioka M., Kato K., Baba T.** Highly polarized electrons from GaAs-GaAsP and InGaAs-AlGaAs strained-layer superlattice photocathodes. *J. Appl. Phys.,* 2005, Vol. 97, p. 94907.

3. **Mamaev Yu.A., Gerchikov L.G., Yashin Yu.P., Vasiliev D.A., Kuzmichev V.V., Ustinov V.M., Zhukov A.E., Mikhrin V.S.** Optimized photocathode for spin-polarized electron sources. *Appl. Phys. Lett.,* 2008, Vol. 93, pp. 81114–81116.

4. **Герчиков Л.Г., Мамаев Ю.А., Субашиев А.В., Яшин Ю.П., Васильев Д.А., Кузьмичев В.В., Жуков А.Е., Семенова Е.С., Васильев А.П., Устинов В.М.** Фотоэмиссия поляризованных электронов из InAlGaAs/GaAsS-сверхрешеток с минимальным разрывом зоны проводимости // Физика и техника полупроводников. 2006. Вып. 11. С. 1361 – 1367.

5. **Brachmann A., Clendenin J.E.; Garwin E.L., Ioakeimidi K., Kirby R.E., Maruyama T., Prescott C.Y., Sheppard J., Turner J., Zhou F.** The polarized electron source for the International Collider (ILC) Project. *AIP Conference Proceedings of 17th International Spin Physics Symposium* (Kyoto, Japan, 2–7 October 2006), 2007, Vol. 915, pp. 1091–1094.

6. **Aulenbacher K., Schuler J., v. Harrach D., Reichert E., Roethgen J., Subashev A., Tioukine V., Yashin Y.** Pulse response of thin III/V semiconductor photocathodes. *J. Appl. Phys.,* 2002, Vol. 92, pp. 7536–7543.

7. **Oskotskij B.D., Subashiev A.V., Mamaev Yu.A.** Polarized photoemission spectra of the strained semiconductors layers. *Phys. Low-Dim. Struct.,* 1997, Vol. 1/2, pp. 77–89.

8. **Герчиков Л.Г., Ауленбахер К., Мамаев Ю.А., Рин Э., Яшин Ю.П.** Транспорт и частичная локализация электронов в короткопериодических напряженных полупроводниковых структурах // Физика и техника полупроводников. 2012. Вып. 1. С. 70 – 89.

9. **Subashiev A.V., Gerchikov L.G., Ipatov A.I.** Optical spin orientation in strained superlattices. *J. Appl. Phys.*, 2004, Vol. 96, pp. 1511–1520.

10. **Matsuyama T., Takikita H., Horinaka H., Wada K, Nakanishi T., Okumi S., Nishitani T., Saka T., Kato T.** High spin polarization of conduction band electrons in GaAs-GaAsP strained layer superlattice fabricated as a spin-polarized electron source. *Jap. J. Appl. Phys.*, 2004, Vol. 43, pp. 3371–3375.

11. **Pusep Yu.A., Chiquito A.J., Mergulhao S., Galzerani J.C.** One-dimensional character of miniband transport in doped GaAs/AlAs superlattices. *Phys. Rev. B,* 1997, Vol. 56, pp. 3892–3895.

ГЕРЧИКОВ Леонид Григорьевич – *кандидат физико-математических наук, доцент кафедры экспериментальной физики Санкт-Петербургского государственного политехнического университета.*

195251, Россия, Санкт-Петербург, Политехническая ул., 29

lgerchikov@rambler.ru

МАМАЕВ Юрий Алексеевич – *доктор физико-математических наук, профессор кафедры экспериментальной физики Санкт-Петербургского государственного политехнического университета.*
195251, Россия, Санкт-Петербург, Политехническая ул., 29
mamaev@spes.stu.neva.ru

ЯШИН Юрий Петрович – *кандидат физико-математических наук, доцент кафедры экспериментальной физики Санкт-Петербургского государственного политехнического университета.*
195251, Россия, Санкт-Петербург, Политехническая ул., 29

КУЗЬМИЧЕВ Виталий Валерьевич – *ассистент кафедры экспериментальной физики Санкт-Петербургского государственного политехнического университета.*
195251, Россия, Санкт-Петербург, Политехническая ул., 29

АУЛЕНБАХЕР Курт – *профессор Института ядерной физики Университета Иоганна Гутенберга.*
55122, Германия, Майнц, Саарштрассе, 21
aulenbac@kph.uni-mainz.de

РАЙХ Эрик – *сотрудник Института ядерной физики Университета Иоганна Гутенберга.*
55122, Германия, Майнц, Саарштрассе, 21